

H. OPTICAL PROPERTIES AT THE APOLLO 16 LANDING SITE

By HENRY E. HOLT

CONTENTS

	Page
Introduction	174
Photometric- studies	174
Procedures	174
Observations	175
Interpretations	181
Polarimetric studies	182
Procedures	182
Observations and interpretations	183
Conclusions	183

ILLUSTRATIONS

	Page
FIGURE 1. Graph showing comparison of telescopically measured photometric function with measured luminances at stations 8 and 13	175
2. Map showing albedo variations within the Apollo 16 site	176
3. Photograph of the Apollo 16 landing site, sun elevation angle 60°	177
4. Computer-generated enlargements of northern, central, and southern areas outlined in figure 2	178
5. Photograph of north wall and southeast rim of North Ray crater and digitized image showing degree of polarization for the same scene	183

INTRODUCTION

The optical properties at the Apollo 16 landing site in the central highlands can be characterized by measurements from surface and orbital photographs. The purpose of this study is to interpret the optical variations over the landing area in relation to the local geology as deduced from the soil and rock samples photographed and collected at the traverse stations. The data provide an opportunity to observe, in some detail, bright rays and older regolith surfaces in the landing site and to compare the optical nature of the Cayley Formation with the adjacent Descartes mountains. Finally, polarimetric studies were conducted with photographs taken through a polarizing filter at two locations on the rim of North Ray crater to determine the degree and orientation of reflected polarized light.

PHOTOMETRIC STUDIES

The brightness reflectances or albedos of materials on the Moon's surface, measured under prescribed lighting conditions, constitute the photometric properties of those materials. Determination of these properties provides an independent method of estimating

the age and composition of texture of lunar surface materials.

PROCEDURES

The Apollo 16 mission provided the first opportunity to test the photometric function of the fine-grained highland regolith for small-scale variations. Photographs taken down-sun, which include the astronaut's shadow allow the measurement of surface reflectance from approximately 50° to near 0° phase angle. Microdensitometer scans were made across photographs taken at stations 6, 8, and 13. The film-density luminances (or percent reflectances) were calculated and plotted relative to phase angle (fig. 1).

Down-sun photographs of the lunar surface at each traverse station were utilized in determining the photometric properties of the undisturbed soil and rock materials. These materials normally appear darker when disturbed. At the Apollo 16 landing site, however, patches of lighter materials were exposed below a thin surface layer at stations 1, 2, 4a, 5, 11, and 13. Surface areas within a few degrees of zero phase angle were scanned by densitometer and the film-density

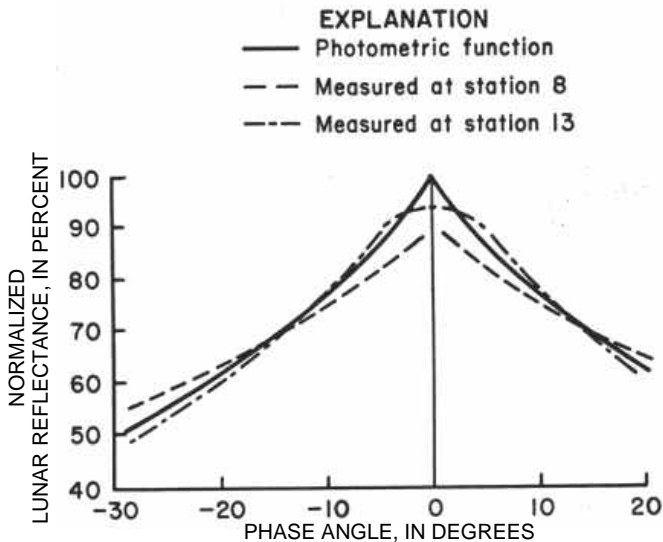


FIGURE 1.-Comparison of telescopically measured photometric function with measured luminances from photographs AS16-106-17386 (station 13) and AS16-108-17702 (station 8).

luminances calculated. The Hasselblad cameras with mm and 500-mm focal length lenses used on the lunar surface were calibrated for variation in film density as a function of absolute light intensities of photographed objects. Photometric control before and after emission was obtained from film measurements of a photometric chart and gnomon photographed on a lunar surface and from film sensitometry data. The camera orientation with respect to lunar azimuth,

lunar vertical, and position of the sun was established on each measurement, and the measured luminances were then converted to 0° phase-angle reflectance for albedo determination. The resultant albedo value of the regolith is the down-sun reflectance expressed as a percentage of the solar irradiance; for instance, 14 percent albedo indicates that 14 percent of the solar light reflected.

Albedo distributions over the Descartes landing area were mapped from orbital panoramic camera frame 328, taken under high sun angle (60° elevation) and 0° forward tilt, producing a 19° phase-angle view of a lunar surface. Relative film densities were digitized on a Joyce-Loebel microdensitometer at a scanning aperture of 50 μ , approximately equivalent to an integrated area of 9 m^2 on the lunar surface. The film densities are proportional to the normal albedos of the lunar surface materials, and the density variations were calibrated to the albedos determined in the down-sun surface photographs at the traverse stations. A photomap showing the distribution of albedo levels as produced by relating appropriate range of digital numbers to quantified albedo levels. Areas of slope

were determined from a topographic map of Descartes landing area (U.S. Army Topographic Command, 1972); slope direction and steepness were computed, and the albedo deviation from a level surface was calculated using the average lunar photometric function. In areas beyond the topographic map coverage, the slopes were compared with known slopes by stereoscopic study to determine slope direction and steepness. The topographic corrections were applied to the albedo levels to neutralize the effects of topographic slopes.

OBSERVATIONS

Slight differences in the slopes of the photometric function curves occur at phase angles near zero, indicating that variations in the backscattering nature of lunar fine-grained materials are minor. The lunar photometric function for mare surface (Holt and Rennison, 1970) is very similar to that of the curves for stations 8 and 13, which is remarkable considering the differences in composition of bedrock. Apparently, the soil textures resulting from the comminution of lunar material by cratering produces the unique backscatter and lunar photometric function while composition controls the albedo.

The albedo map of a 500- km^2 area (fig. 2) can be compared with an orbital photograph at similar scale (fig. 3). The mapped area is dominated by the two bright areas of North Ray and South Ray craters and their radiating ejecta patterns. Map units 6 and 7, representing albedo levels of 11 through 15 percent, cover more than 58 percent of the mapped area. Where map unit 5 occurs, representing 15 to 17 percent albedo, there is nearly always clear evidence of relatively recent, bright small craters or diffuse ray patterns. The more clearly radial, diffuse to discontinuous bright ray material from North Ray and South Ray craters makes up unit 4, which ranges from 17 to 20 percent normal albedo. Map unit 3, ranging from 20 to 25 percent albedo, represents continuous to discontinuous streaks of ejecta from South Ray crater, both raylike patterns and continuous ejecta from North Ray crater, and rim deposits on many smaller craters. The rim deposits of North Ray crater and the outer parts of the continuous ejecta from South Ray crater make up map units 1 and 2, varying from 25 to 40 percent albedo. The unit with the highest reflectance, about 40 to 60 percent normal albedo, makes up most of the crater wall of North Ray crater, the wall, rim, and some continuous ejecta of South Ray crater, and the rim and wall of Baby Ray crater.

The albedos of the fine-grained regolith at the traverse stations in the Descartes landing area range from 14 to 32 percent. The albedos of the regolith at the

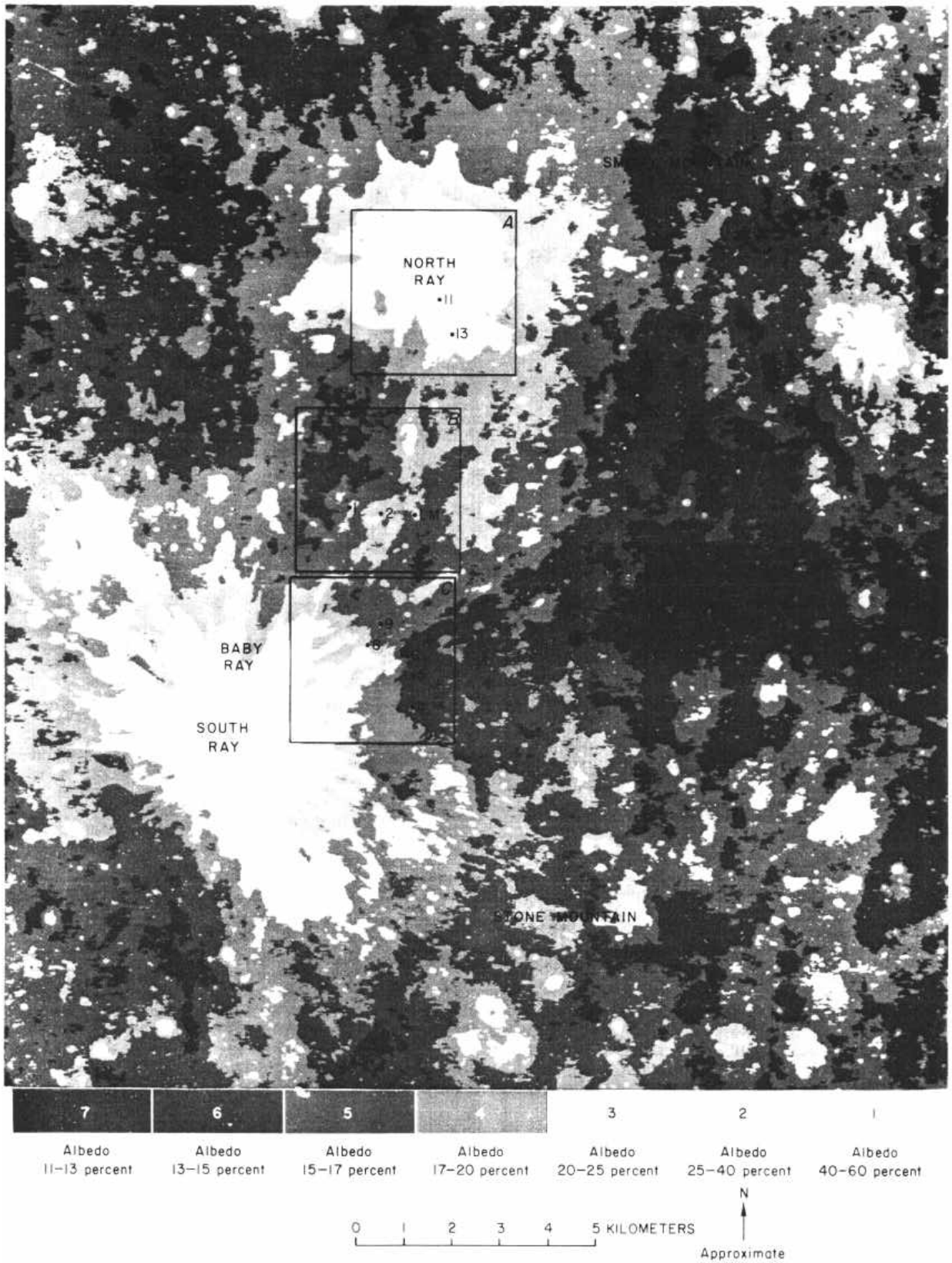


FIGURE 2.- Albedo of the Apollo 16 site based on Apollo 16 panoramic camera frame 5328. Normal albedos, divided into seven percentage ranges, are shown by the gray scale. Enlargements of areas A, B, and C are shown in figure 4. Numbered localities are station, on EVA traverses. Albedo corrections were made for topographic slope elements measured on the premission topographic map (U.S. Army Topographic Command, 1972).

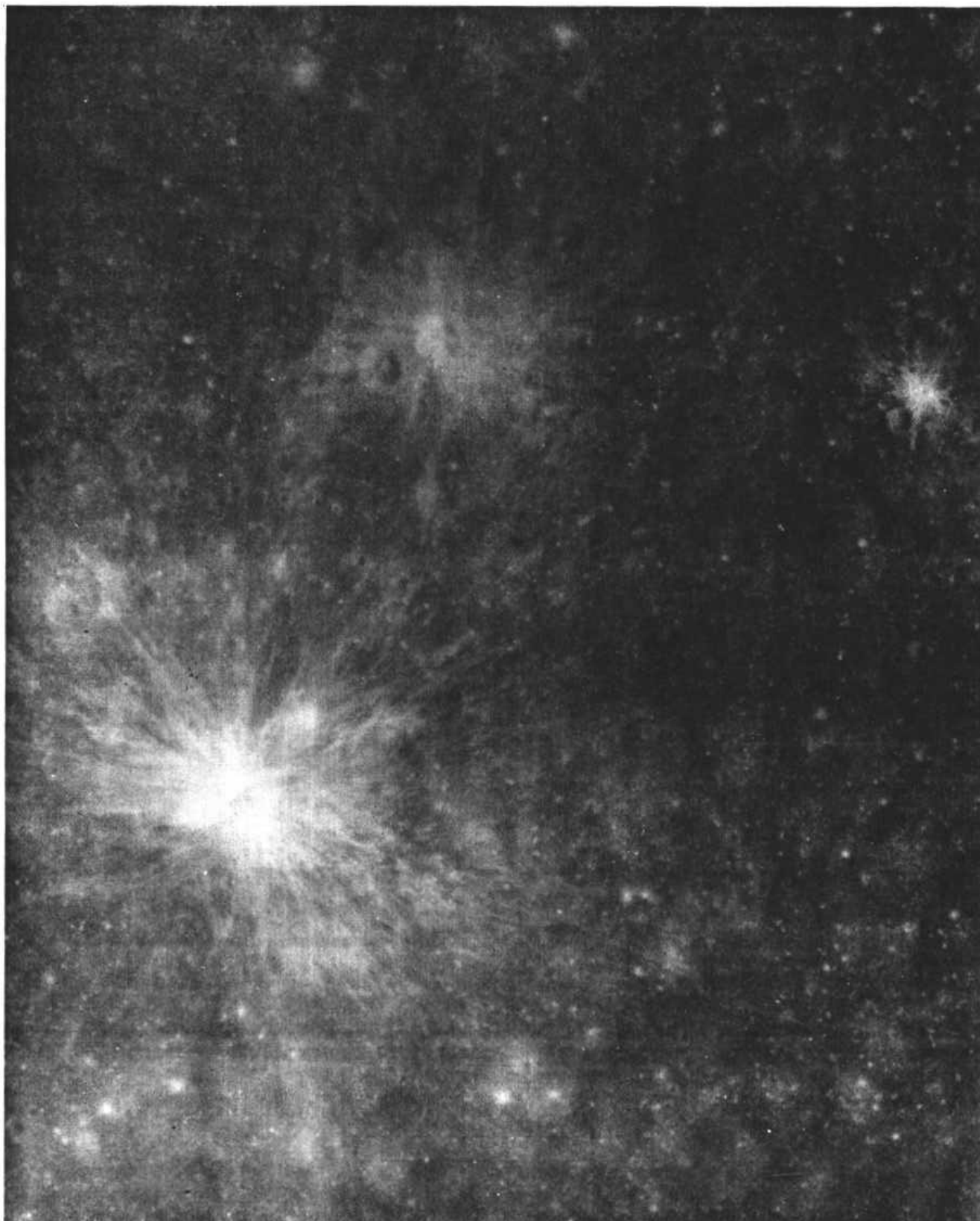


FIGURE 3.-The Descartes landing area as viewed on Apollo 16 panoramic camera frame 5328. Scale of photograph is same as albedo map of figure 2. Sun elevation 60° , camera tilt 10° from vertical toward the west, producing a phase angle of 19° .

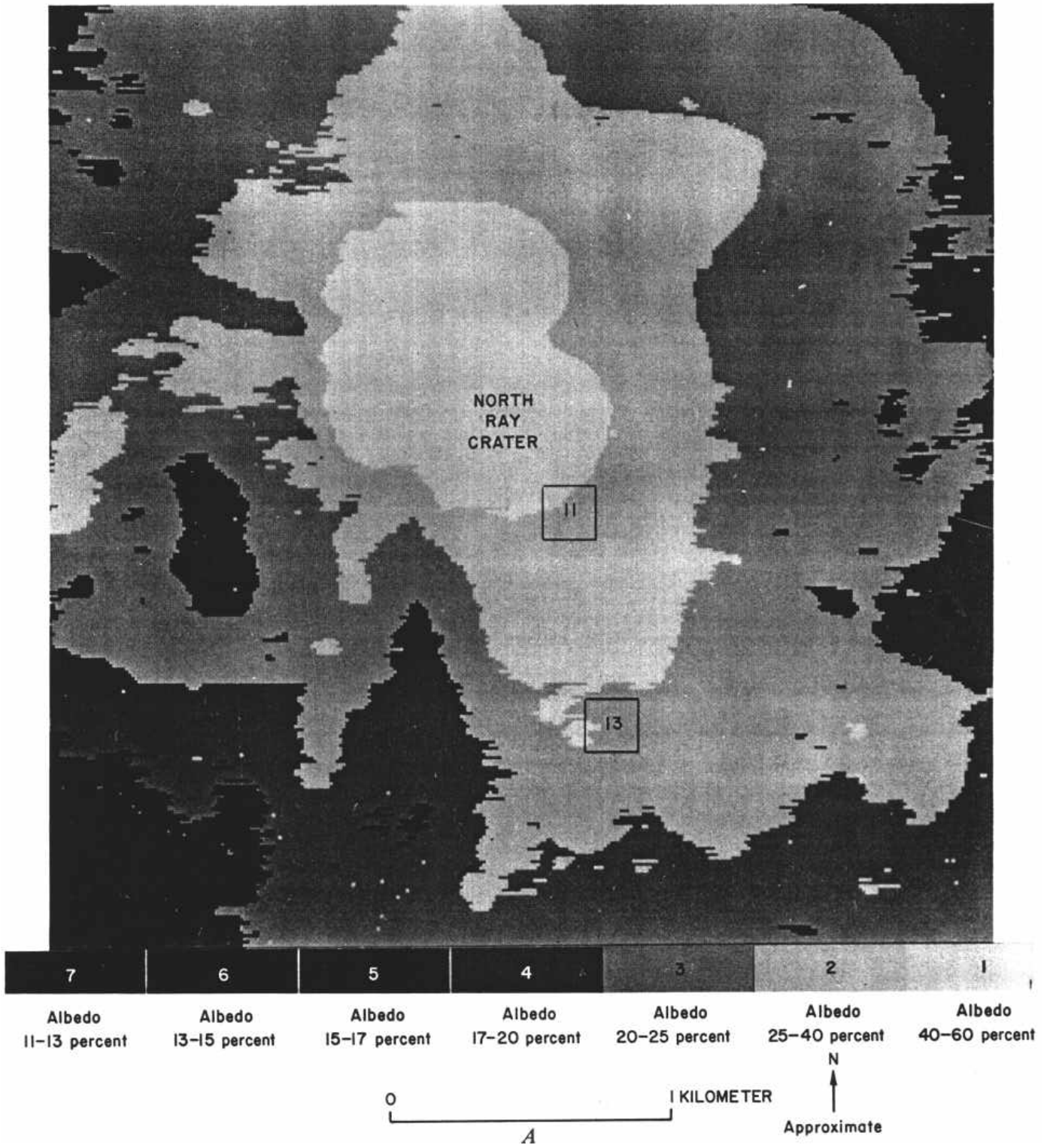


FIGURE 4.-Computer-generated enlargements of areas A, B, and C outlined in figure 2. Station locations identified by number inside scribed areas. Gray shades represent same ranges as given in figure 2. A, Area A. B, Area B. C, Area C.

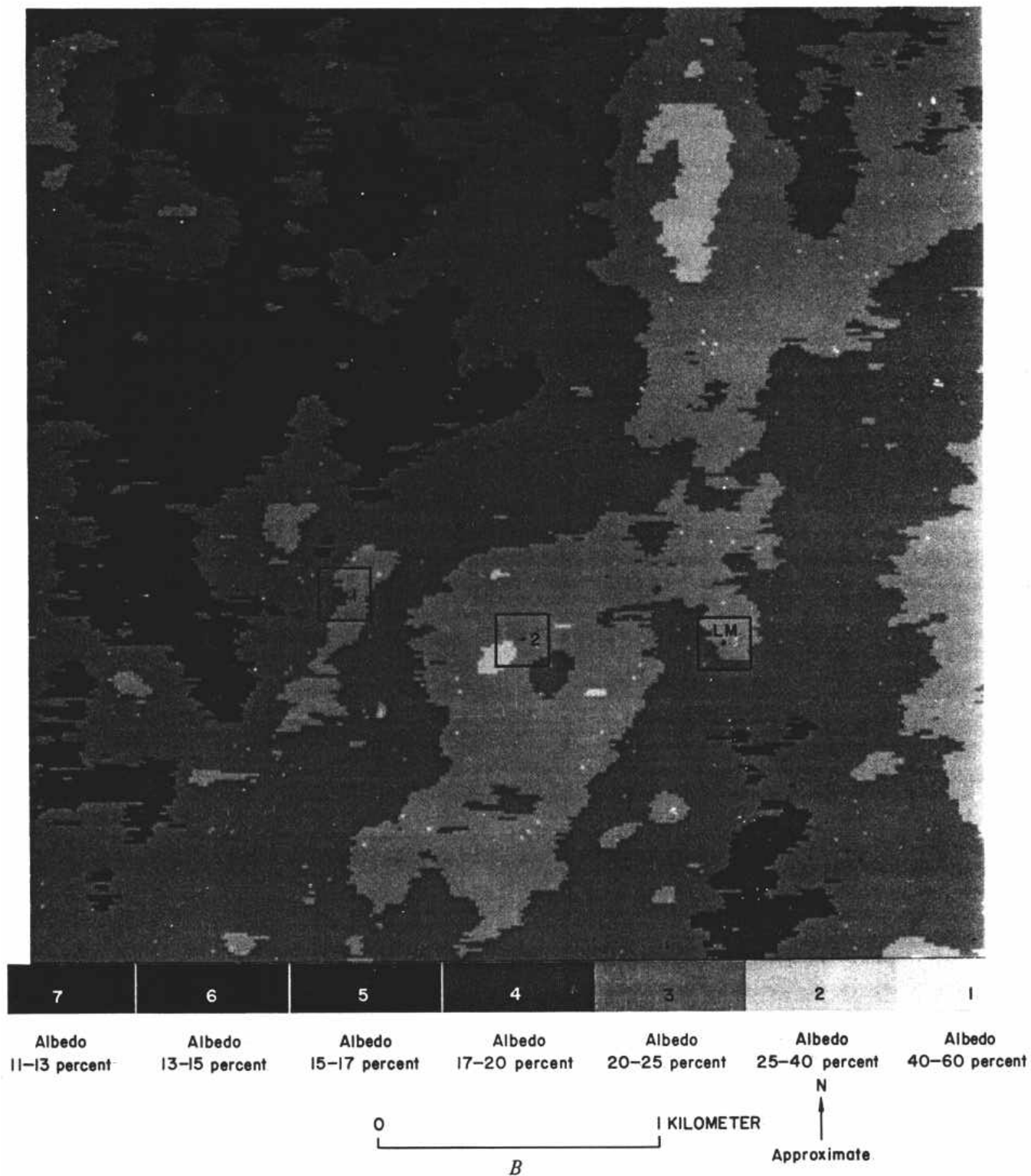


FIGURE 4.-Continued.

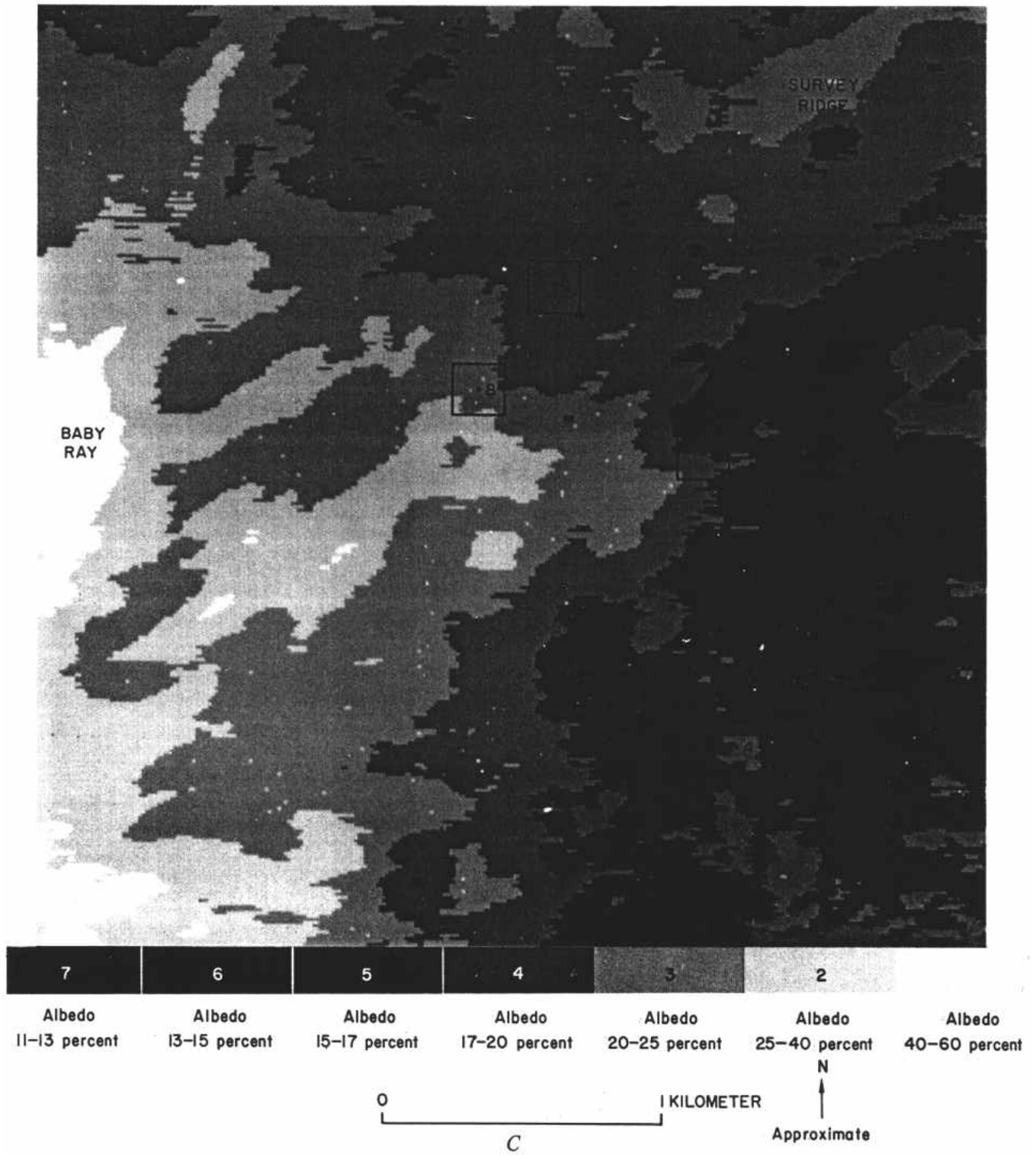


FIGURE 4.-Continued.

traverse stations fall into three groups (fig. 2) that appear to be controlled by proximity to North Ray and South Ray craters. Stations 11 and 13 (fig. 4A) are situated on the bright North Ray crater ejecta and exhibit albedos of 21 to 32 percent. The albedos of stations 1, 2, 6, 8, 9, and LM vary from 16 to 19 percent over the discontinuous ray area between North Ray and South Ray craters. Stations 4 and 5 on Stone mountain show 14 to 15 percent albedo. Rock measurements vary from 18 to 51 percent; the brightest rocks are the light-matrix breccias on the rim of North Ray crater. The bright raylike materials on the rim of South Ray crater reach a maximum albedo of 60 percent, the brightest materials on the walls of North Ray crater 52 percent. These high albedos are more than twice the highest telescopically measured lunar albedo of 24 percent on the crater walls of Aristarchus (Pohn and Wildey, 1970). The extremely wide range of albedos, 14 to 60 percent, is the greatest of any lunar landing area. The high values stem from the high resolution possible with lunar surface photography relative that from a telescope.

INTERPRETATIONS

Units 1, 2, 3, and 4 on the albedo map can be clearly related to ejecta from identifiable craters. Unit 5 is traceable around isolated craters, forming a pattern radiating from South Ray and North Ray craters, and occurs as small diffuse irregular patches of probable ejecta. Albedo units 6 and 7 represent the more mature regolith surface where lighter subsurface materials have not been excavated or recycled to the surface for a long period of time.

The albedo map does not indicate any measurable differences between the optical properties of the regolith overlying the Cayley Formation and the regolith on Descartes materials of Stone and Smoky mountains. The range of albedo values over both areas is similar, suggesting that there is no significant difference in gross chemical composition of the regolith materials. Soil samples collected from both the Cayley Formation and Stone mountain are reportedly similar in chemical composition (LSPET, 1972) although their percentages of agglutinates, glasses, mineral, and lithic fragments vary. The regolith over the Apollo 16 area may be heterogeneous on a local scale; it becomes more homogeneous on a regional scale, presumably through the maturing action of the repetitive small cratering events. The chemical and optical properties of the more mature soil areas suggest that the regolith over the Cayley plains and Descartes mountains was derived from a similar suite of rocks.

Soil samples obtained from traverse stations consist of various mixtures of agglutinates, glassy fragments,

light-colored lithic fragments, and dark lithic fragments (Heiken and others, 1973). As a soil "ages" or matures on the surface, it becomes darker, the agglutinate content increases, and the soil becomes finer grained (Adams and McCord, 1973). The soils from stations 4 and 5 are the darkest, having the highest agglutinate content and the smallest average grain size of the traverse stations. Lighter soils (stations 11 and subsurface 1) are coarsest, have a higher percentage of light-colored lithic fragments and the lowest percentage of agglutinates.

Soils at the other stations are intermediate between the lighter and darker soils and could be considered mixtures of the two types. The lighter soils at station 11 are immature soils of North Ray crater ejecta; samples of soils collected in areas of high-albedo ray patches (station 8, map unit 4) are not clearly derived from South Ray crater. The coarser fractions, lighter color, and lower proportion of agglutinates in the soils from stations 1, 2, and 6 suggest the contamination, probably by South Ray fine-grained ejecta, of a more mature preexisting soil at these locations.

The combination of surface photographs, crew observations, soil samples, and albedo mapping from orbital pictures permits a detailed study of the character of recent ray ejecta and provides insights into the aging process of rays. The crew recognized discontinuous ray patches as concentrations of rock fragments on the surface along linear trends. Changes in albedo were not noticed near the edge of a ray patch, and no characteristic of the fine-grained regolith was described that could identify ray areas. The rock fragments in ray areas were mainly less than 5 cm across; they covered from less than 1 to as much as 7 percent of the surface area, with the most frequent size range comprising 2 to 5-cm cobbles (Muehlberger and others, 1972). The interray and ray areas delineated on orbital photography generally appear to have similar fragment frequency in the high-resolution surface photograph although local ray segments identified on the surface are not necessarily visible on orbital photographs.

The lighter colored ray materials gradually darken, by an aging process that must be similar to regolith darkening, until their surfaces become indistinguishable from adjacent interray areas. The upper surface of ray material will darken with increase in agglutinate and reduction of the average grain size as well as by mixing with darker preray regolith, both laterally and from below. Gardening by numerous small impact cratering events has been estimated to take 10 m.y. to turn over the uppermost centimeter at least once (Gault and others, 1974). The occurrence of 2-3 cm of darker soil overlying lighter material at stations 1, 2, 6, 11, and 13 is reasonably consistent with a North Ray crater source 50 to 60 million years ago. South Ray

crater fine-grained ejecta would be expected to show little aging in 2 to 4 m.y.

POLARIMETRIC STUDIES

The polarimetric properties of rocks and soils at North Ray crater were investigated to determine the degree and orientation of polarized light reflected from those materials in the north and northeast crater wall. Measurements of these properties help to establish the abundance of brecciated rocks and the lack of crystalline material at that location.

On the high-sun (19° phase angle) Apollo 16 orbital pictures, individual rays from South Ray crater can be observed to extend at least 10 km northward, overlapping North Ray ejecta west and southeast of North Ray crater. Rays become slightly discontinuous about 3 km from South Ray crater. Rays extend eastward over Stone mountain as far as 7 km from South Ray crater. Continuous ejecta and rays from North Ray crater appear to extend only 3 km and 5 km; respectively. This more restricted distribution may result from the greater age of North Ray crater (50 m.y., Walton and others, 1973) compared with South Ray crater (2-4 m.y., McKay and Heiken, 1973) and consequently greater mixing; and aging of the ray materials. North Ray crater excavated more than three times as much material as South Ray crater, and its ejecta must have been scattered over a significantly larger area than covered by the present distribution of visible South Ray crater ejecta. Most of the traverse area should have been nearly continuously covered by North Ray ejecta and ray materials. Lighter materials were observed 2 to 3 cm below a darker gray surface layer at many stations and may represent North Ray crater ejecta.

The rays are features that become more visible as the phase angle approaches zero (also referred to as the opposition effect), a property of fine-grained materials. Those rays that become most visible at opposition contain a higher proportion of light soil. Rock fragments show a Lambertian type reflectance, greatest relative to the fine-grained regolith at 30° to 50° phase angle. Surface fragments tend to reduce the overall opposition effect except where the fragments are covered by a dust layer. As described by Muehlberger and others (1972), rock-fragment concentrations are commonly similar in ray and interray areas; hence the light soils must be the controlling factor. Several areas of rock concentration were considered rays by the crew, but those areas do not exhibit consistently high albedo at low phase angles, indicating that light soil is not present (station 4 and 5 are examples). In one of the brightest areas crossed, Survey ridge, albedo 24 percent, as much as 7

percent of the surface is covered by fragments larger than 2 cm (Muehlberger and others, 1972; Schaber, this volume, fig. 2). A similar concentration of fragments occurred near station 5, where the soil albedo was 14 percent compared with 24 percent at Survey ridge. The ray patterns are visible at low phase angles only because lighter colored fine-grained material occurs as ray material, with or without any concentration of rock fragments.

PROCEDURES

A polarizing filter attached to the lunar surface Hasselblad camera permitted measurement of the degree of polarization and the orientation of the plane of maximum polarization of light reflected from the lunar surface. Three photographs were needed, one each with the polarizing filter at the 0 , 45 , and 90° positions. To obtain the data needed, overlapping photographs were taken at one filter position through a 120° sector across North Ray crater from station 11. The filter was then rotated to the second position and the sector rephotographed. This was repeated a third time in the final filter position. Differences in image intensity of the same image element or object in the three photographs are a function of the amount and orientation of the linear component of polarized reflected light from that object.

Three sets of polarization frames were selected for computer processing from the returned photographs: frames AS16-106-17239, 17241, 17257, 17259, 17266, and 17268 from the southwestern panoramic position at station 11, and frames AS16-106-17283, 17296, and 17310 from the northeastern panoramic position at station 11. The data for computer reduction were taken from second-generation master positives. The sets of photographs were digitized and the frames filtered using a 3- by 3-pixel matrix to smooth the data. The first frame (horizontal polarization) became the prime photograph against which the remaining two were registered. Camera displacements between frames were sufficiently large to yield stereopairs from frames within a given set. Registration of stereopairs to pixel resolution is extremely difficult and requires lengthy computer processing. To reduce expensive computer time, a special set of positive transparency enlargements of the digitized photographs was made. The frames were then registered visually and displacement coordinates were determined for 70 to 80 points in each frame. These point displacements were used to compute linear interpolation of the displacement coordinates. This interpolation factor was applied to each photograph element. The registrations, while still imperfect, were within 5 pixels in the far field.

The three registered frames were used to compute

light fragmental soil, destroying the typical ray structure. Most of the continuous to discontinuous ray materials merged into a diffuse halo around North Ray crater having albedos of 25 to 30 percent on the rim deposits, decreasing outward to 16 to 18 percent as far as 8 km away.

The South Ray crater event, 2 to 4 million years ago, scattered light subsurface material over much of the traverse area. The light discontinuous patches of ray materials are visible, in the author's opinion, because of the light fine-grained component of the ejecta rather than the fragment population (2-7 percent of area) over the surface of a ray. The Baby Ray impact event scattered more light-colored subsurface material over distances of a few kilometers. The surficial gardening processes should have had little effect in altering or darkening ray materials from South Ray and Baby Ray craters. The surface albedo patterns over the Descartes area are produced by a combination of the older North Ray and the younger South Ray and Baby Ray ejecta deposits and the preexisting nearly uniform regolith

surface. Bright, continuous-to-discontinuous ejecta (albedo units 1, 2, 3, and 4) cover 23 percent of the mapped area. More diffuse lightened regolith (unit 5) in patterns radial to North Ray and South Ray craters occupies more than 18 percent of the area and probably represents a mixture of light ejecta with preexisting regolith.

The rocky surfaces around North Ray crater rim and within the crater wall contain little crystalline material that can polarize reflected light. The polarimetric properties of these rocks suggest that they are much more highly shocked than the Aura Mauro breccias from Cone crater at the Apollo 14 site. No areas, layers, or blocks of intermediate to strong polarization such as would be expected for relatively unshocked basaltic crystalline rock were observed. On the basis of unpublished laboratory measurements on crushed anorthosite, all measurements at North Ray crater are consistent with the polarimetric properties of highly brecciated and shocked material of predominantly anorthositic composition.